ACS Photonics

Article

Cite This: ACS Photonics 2018, 5, 4529−4537

pubs.acs.org/journal/apchd5

Importance of Evaluating the Intensity Dependency of the Quantum Efficiency: Impact on LEDs and Persistent Phosphors

David Van der Heggen, Jonas J. Joos, and Philippe F. Smet*

LumiLab, Department of Solid State Sciences, Ghent University, Krijgslaan 281 S1, 9000 Gent, Belgium

ABSTRACT: The quantum efficiency is a key metric in lighting technology and for the quantification of luminescent processes, indicating how many photons are emitted with respect to the number of absorbed photons. Ideally, this value should approach unity to reduce losses, for instance in the common phosphor converted white LEDs. In this work we demonstrate that in luminescent materials where energy can be stored at defect centers, like in the extreme case of persistent phosphors, the quantum efficiency depends on the excitation intensity. For the green emitting $SrAl_2O_4:Eu^{2+},Dy^{3+}$, which has been proposed for use in AC-LEDs, the internal quantum efficiency drops for increasing excitation intensity from 71% to 54%. At elevated excitation intensities, as encountered in LEDs, the trapped charge carriers can be optically detrapped by the excitation light, leading to this strong reduction of the overall quantum efficiency. Considering that the absorption cross section for this process is 6−29× larger than the absorption cross section for the luminescent ion, the efficiency of LED phosphors can be increased by avoiding the presence of defects acting as trapping centers. Finally, designing persistent phosphors with defects that show a limited optical response for the excitation light could strongly increase their energy storage capacity.

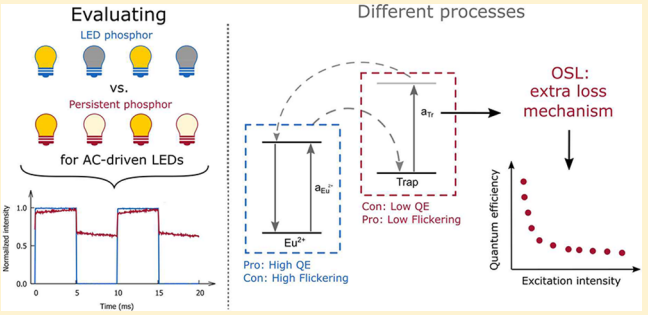

KEYWORDS: *strontium aluminate, persistent luminescence, optically stimulated luminescence, storage capacity, quantum efficiency*

Phosphors are a key component in modern white light-emitting diodes (LEDs).[1−5] These luminescent materials convert the monochromatic light from the blue or ultraviolet pumping LED into other colors, the combination of both resulting in white light. Typical decay times of LED phosphors range from several tenths of nanoseconds to several milliseconds, so continuous light emission can only be obtained if the pumping LED emits light uninterruptedly. To accomplish this, the LEDs are equipped with driver electronics which are commonly incorporated in the LED packaging and convert the alternating current (AC) into direct current (DC).[6] These driver electronics are however often susceptible to failure and limit the lifespan of the LED lamp. To avoid this problem it was proposed to switch to AC-driven LEDs.[7,8] Even though this approach improves the durability of an LED, the alternating current introduces a new problem as the LED is reverse biased during 50% of the time causing it to switch on and off at a frequency of 100 to 120 Hz. This fluctuation in the light intensity, a phenomenon generally referred to as flickering, is considered to be a health hazard.[9]

Flickering can be reduced by using phosphors which decay slowly, such as many Mn-based phosphors, which have typical decay times of several milliseconds.[10−13] This slow decay bridges the dark periods in which the LED is switched off, thereby reducing the flickering. But long decay times are often accompanied by saturation effects.[1] These saturation effects manifest themselves at high excitation fluxes as a sublinear increase in the emission intensity and a decrease in the overall absorption of the phosphor.[10,14,15] This can lead to color variations with varying excitation intensities, which is clearly an unwanted effect.

A solution to this problem can be found in the recently proposed idea to use persistent phosphors in AC driven LEDs.[16−24] These persistent phosphors are different to ordinary conversion phosphors as they exhibit light emission that persists seconds to hours after the excitation has stopped.[25] The reason for this delayed emission is their ability to store energy in the material, presumably at defects other than the luminescent ion. These defects are called traps because a charge carrier originating from the luminescent ion is locally trapped at the defect.[26−30] When sufficient energy is provided to the trapped charge it will be released. After recombination at the luminescent ion, it will give rise to the delayed emission that is generally referred to as afterglow. The timespan of the afterglow can be tuned, as it depends on the so-called depth of the trap, which is typically probed by thermoluminescence.[31] For most applications, such as safety signage, road markings,[32] or bioimaging,[33−36] the afterglow time should be of the order of hours. However, for lighting applications, this should be of the same order of magnitude as the dark time, so the trap should be sufficiently shallow to achieve afterglow times of a few hundreds of milliseconds. The

Received: July 18, 2018
Published: October 12, 2018

DOI: 10.1021/acsphotonics.8b00979
ACS Photonics 2018, 5, 4529−4537

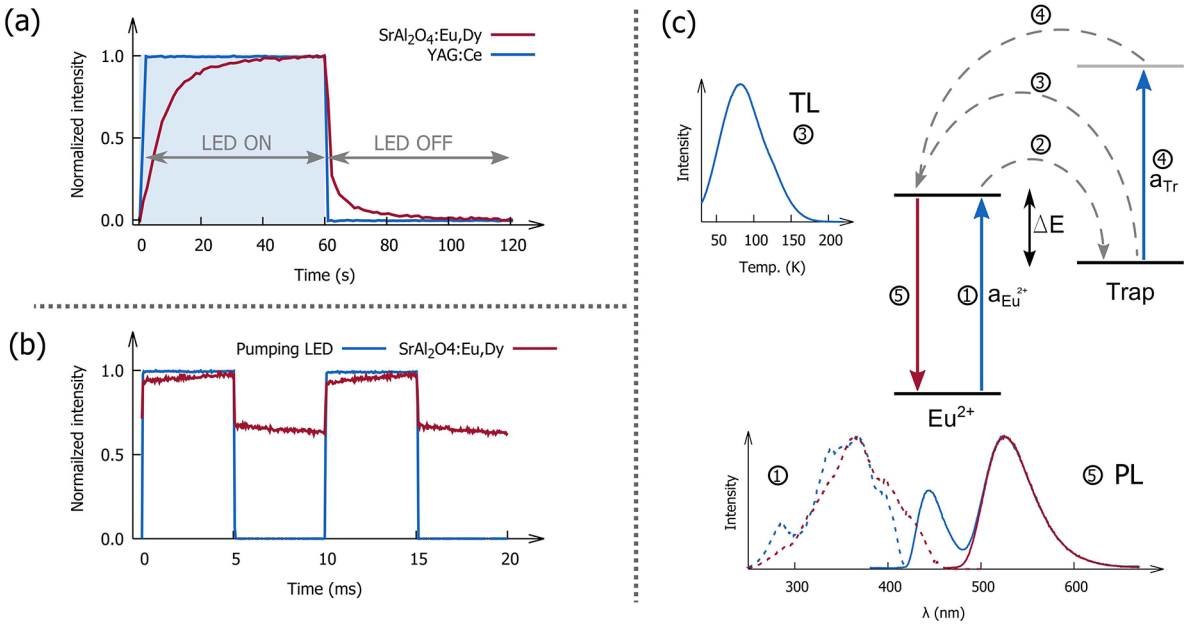

Figure 1. (a) Illustration of the time scale of the different processes in persistent ($SrAl_2O_4:Eu^{2+},Dy^{3+}$) and LED phosphors ($Y_3Al_5O_{12}:Ce^{3+}$). (b) The extent to which flickering is reduced by $SrAl_2O_4:Eu^{2+},Dy^{3+}$.(c) Schematic representation of the different processes that take place in a persistent phosphor. The solid arrows represent optical transitions, while nonradiative transitions are represented by dashed arrows. The photoluminescence (PL) emission and excitation spectra (measured at 10 K) and the thermoluminescence (TL) glow curve are shown in the insets.

presence of trapping defects is, however, not always intentional, as they can also be accidentally incorporated during synthesis of the more common LED phosphors. The characteristics of these traps might be such that they do not induce afterglow at room temperature, making it difficult to detect their presence. This does, however, not mean that the presence of trapping defects does not alter other properties such as the phosphor's quantum efficiency or the thermal quenching behavior.[37,38]

Overall, LED phosphor research aims at improving the efficiency and color quality of the resulting phosphor converted LEDs.[1,39] In addition to the inevitable Stokes losses, current phosphor quantum efficiencies are still responsible for a significant fraction of all the heat losses in LEDs,[40] and further optimizing the phosphor's quantum efficiency still offers room to enhance the overall efficiency of a white LED. An LED phosphor needs to have a high quantum efficiency and it needs to be able to withstand high temperatures[37] and high illumination intensities.[1] The last two requirements deserve special attention in case traps are present in the phosphor, as the release of trapped charge carriers can be provoked by the elevated temperatures and high excitation fluxes that are typically encountered in LEDs.[15] Here, it is shown that optically induced detrapping by excitation light results in a dramatic decrease of the quantum efficiency and a simultaneous increase in the absorption strength of the persistent phosphor, a trend that is generally not encountered in LED phosphors. In this work we will demonstrate the extent of this effect and the implications for research on LED and persistent phosphors.

METHODS

All measurements were performed on 50 mg of commercial $SrAl_2O_4:Eu^{2+},Dy^{3+}$ powder (GloTech Inc.), which was incorporated in a polymer layer (diameter 18 mm) as described in previous work.[41] Quantum efficiency and absorption measurements were performed in an integrating sphere[42] (LabSphere GPS-SL series) under excitation with a blue LED with a central wavelength of 445 nm and a full width at half-maximum (fwhm) of 20 nm or a UV LED with a central wavelength of 375 nm and a fwhm of 15 nm. The spectra were recorded using a ProEM 1600 EMCCD camera attached to an Acton SP2300 monochromator (Princeton Instruments). The setup was calibrated using deuterium and halogen calibration lamps (DH-2000-CAL, Ocean Optics). Luminescence decay measurements were conducted using a pulsed blue LED (445 nm) as excitation source and a gateable and intensified CCD (Andor iStar) attached to a Jarrel-Ash monochromator. The afterglow measurements used to determine the storage capacity were recorded with an ILT 1700 calibrated photometer (International Light Technologies) equipped with a photopic filter (YPM). A FLIR A35sc infrared camera was used to measure the sample's temperature. Diffuse transmission spectra were recorded using a Varian Cary 500 UV−vis−NIR spectrophotometer equipped with a 110 mm $BaSO_4$-coated integrating sphere. For the determination of absorption cross sections, diffuse transmission spectra of a polymer layer with a lower phosphor loading of 8 mg/cm^2 were used.

RESULTS AND DISCUSSION

The internal quantum efficiency of a luminescent material is usually defined as[1]

$$\eta_{in} = N_{em}/N_{abs} \quad (1)$$

where N_{em} and N_{abs} represent the number of emitted and absorbed photons, respectively. This is in contrast to the quantity represented in an excitation spectrum, which corresponds to the external quantum efficiency, where the number of emitted photons is compared to the number of incident photons. Here, we will not be concerned with the

DOI: 10.1021/acsphotonics.8b00979
ACS Photonics 2018, 5, 4529−4537

latter, and for the sake of brevity, the term quantum efficiency will be used for internal quantum efficiency in the remainder of the text. Even though eq 1 seems straightforward, it is imperative that a distinction is made between the internal quantum efficiency at the level of the luminescent ion or at the level of the phosphor. In the former definition, N_{abs} corresponds to the number of photons absorbed by the luminescent ion, whereas for the latter it is defined as the number of photons absorbed by the complete phosphor. In this work we will be concerned with the second definition. In case no trapping occurs, the internal quantum efficiency corresponds to the efficiency of the photoluminescence process, provided that no additional absorption occurs due to detrimental defects or impurity phases. However, once traps are present in a phosphor, additional effects like trapping, afterglow, or optically stimulated luminescence can take place. These processes are schematically represented in Figure 1c. All of these processes start with the absorption of a photon (1) exciting the activator. If the activator immediately relaxes to the ground state by emission of a photon (5), it is called photoluminescence. Alternatively, excitation can be followed by a transfer of energy to a trapping defect (2), which presumably happens by exchanging a charge carrier.[27−29] If energy is provided to this trapped charge carrier, it can be released and recombine at the activator (5). If the detrapping is thermally stimulated (3), the process is called persistent luminescence or afterglow if the temperature is constant, or thermoluminescence (TL), when the temperature is (typically linearly) increased. If, on the other hand, the energy is provided by the excitation light (4), the process is called optically stimulated luminescence (OSL). In Figure 1a, the behavior under pulsed excitation of a typical LED phosphor such as $Y_3Al_5O_{12}:Ce^{3+}$ (YAG:Ce) is compared to the persistent phosphor $SrAl_2O_4:Eu^{2+},Dy^{3+}$. While the YAG:Ce phosphor perfectly follows the emission profile of the blue pumping LED, the $SrAl_2O_4:Eu^{2+},Dy^{3+}$ persistent phosphor shows an increase when the blue light is switched, a so-called charging behavior, followed by a rather exponentially decreasing afterglow. When reducing the pulse width to 5 ms, nothing changes for the YAG:Ce, due to its short photoluminescence decay time of 65 ns.[43] As the off-time of only 5 ms is not sufficient to fully deplete the traps in the $SrAl_2O_4$:Eu,Dy persistent phosphor in between pulses, a fairly constant emission is found, effectively reducing flickering. It is clear that these additional processes in persistent phosphors take place on much longer time scales than the photoluminescence so that steady state equilibrium conditions are required to unambiguously define the quantum efficiency for these materials.

In an attempt to quantify the extent to which these additional processes affect the performance of the phosphor, the internal quantum efficiency of $SrAl_2O_4:Eu^{2+},Dy^{3+}$ was measured as a function of the excitation intensity. The results are displayed in Figure 2. Both for excitation with 375 and 445 nm the quantum efficiency undergoes a steep decrease before leveling off. This is in stark contrast with the internal quantum efficiencies of LED phosphors which, in the absence of saturation effects, are independent of the excitation intensity. In case of 445 nm excitation, the quantum efficiency is 71% for low excitation intensities, but levels off at 54% when the intensity is increased. The latter value is in reasonable agreement with the value of 44% found in literature.[44] The quantum efficiency under 375 nm excitation is however much

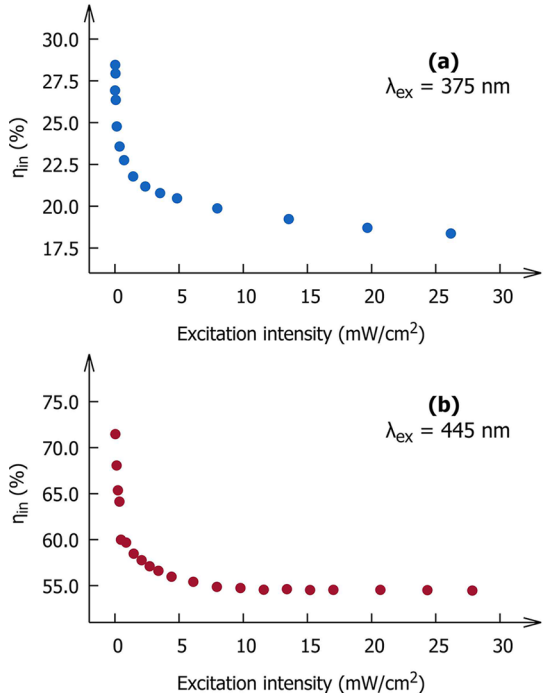

Figure 2. Intensity dependence of the internal quantum efficiency of $SrAl_2O_4$:Eu,Dy under excitation with ultraviolet (a) or blue (b) light.

lower, around 28% for the lowest intensities, leveling off at a value of 18%. This wavelength dependence can be understood from the fact that $SrAl_2O_4:Eu^{2+},Dy^{3+}$ accommodates Eu ions on two different crystallographic sites.[45,46] This is known to give rise to two different emission bands: a blue emission band peaking at 445 nm, which is fully quenched at room temperature,[47] and a second band that is centered around 520 nm and is responsible for the material's well-known green emission.[45,46,48] While 445 nm light can only excite the site responsible for the green emission, 375 nm light excites both sites, which might further complicate the matter at hand.

One might presume that the decreasing quantum efficiency with increasing excitation intensity is due to thermal quenching. This argument was taken under consideration as the phosphor could indeed heat up during illumination due to Stokes losses or nonradiative decay. It is well-known that thermal quenching is accompanied by a decrease of the decay time[43] so in order to test this hypothesis decay profiles were measured as a function of the excitation intensity. It was reported that the photoluminescence decay of $SrAl_2O_4:Eu^{2+},Dy^{3+}$ contains two components[45] and, in this case, the derived decay times are (200 ± 35) and (720 ± 50) ns. Figure 3 shows that these decay times remain largely unaffected as a function of excitation intensity, showing that thermal quenching is not responsible for the observed decrease in the quantum efficiency. This was confirmed by a thermal imaging camera showing no higher temperature increases than 1 °C for the highest excitation intensities.

The intensity dependence of the quantum efficiency can be explained by assuming that the trapping and detrapping processes in persistent phosphors have a different intensity dependence as well as a different quantum efficiency. From this point of view, OSL induced by excitation light is of special interest: as illustrated in Figure 1c, two photons (1, 4) need to be absorbed to yield emission of a single photon (5). Based on eq 1 it can be concluded that the internal quantum efficiency of

DOI: 10.1021/acsphotonics.8b00979
ACS Photonics 2018, 5, 4529−4537

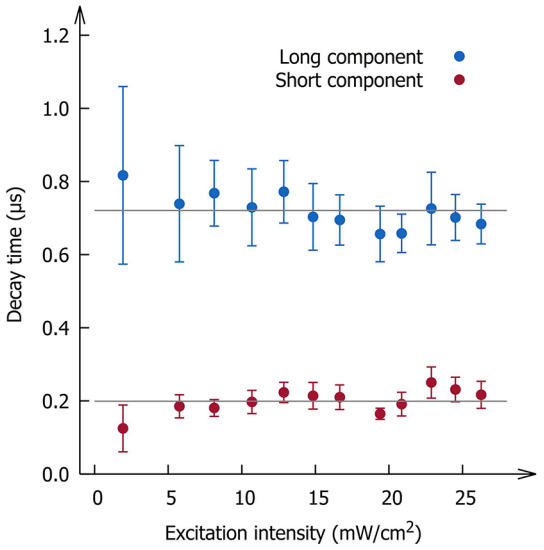

Figure 3. Intensity dependence of the decay times of the Eu^{2+} emission in $SrAl_2O_4:Eu^{2+},Dy^{3+}$ excited by 445 nm light at room temperature. The averages are indicated by the gray lines and correspond to (720 ± 50) and (200 ± 35) ns.

such a process is capped at 50%, regardless of the nonradiative pathways to which it might be subjected. It is important to stress that, in contrast to other two-photon processes, such as upconversion,[49,50] OSL can also occur at low excitation intensities due to the long lifetime of, what could be called, the intermediate state.

Evidence to support this hypothesis can be found in the thermal quenching profile of $SrAl_2O_4:Eu^{2+},Dy^{3+}$ under 435 nm excitation, as measured by Botterman et al.[45] (see Figure 4). This profile is quite unconventional, as it exhibits an additional drop in intensity around 220 K before thermal quenching sets in around 450 K, irrespective of whether the profile is measured while heating up or cooling down. The temperature of this first drop corresponds to the temperature at which

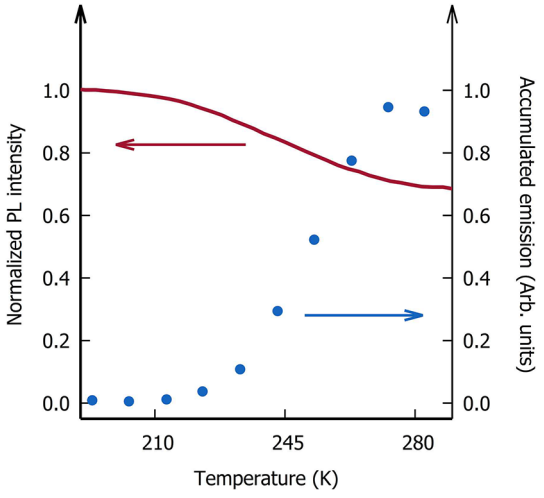

Figure 4. Temperature dependence of the photoluminescence intensity of $SrAl_2O_4:Eu^{2+},Dy^{3+}$ under 435 nm excitation (red line) and the accumulated emission intensity during afterglow and thermoluminescence (blue dots), being a measure for the total amount of filled traps at the end of the excitation with 435 nm. Figure adapted, with permission, from Botterman et al.[43]

trapping becomes thermally activated (see Figure 4), suggesting that this yet unexplained drop is a consequence of OSL by excitation light. However, trapping is not always thermally activated, and if it takes place at lower temperatures as well, the effect on the thermal quenching profiles will be more difficult to detect. Rather than exhibiting a dip in intensity, it is expected that the thermal quenching profiles of these phosphors will start at a lower intensity than the intensity of a similar phosphor without trapping centers.[51] An interesting class of phosphors to be considered in this case are those in which the traps are engineered in such a way that the thermal stability is enhanced.[37,38] For these phosphors it should be investigated case per case whether the enhanced thermal stability is worth compromising the phosphor's quantum efficiency.

To further demonstrate the importance of the OSL mechanism on the phosphor performance the absorption is studied in more detail. The absorption is measured in the integrating sphere by illuminating the phosphor layer with light of a specific wavelength and then calculating the fraction of the incident light which is absorbed by the phosphor. Figure 5a,c shows that an intensity dependence is also found here, with an increase from 23% to 28% at 445 nm for increasing excitation intensities. At 375 nm, a similar trend is found, but the absorption is about 4× higher due to the increased absorption of Eu^{2+} at this wavelength (Figure 6). The increase of the absorption with increasing excitation intensity is unusual since for LED phosphors the absorption is expected to either remain constant or decrease if saturation effects take place.[10,14]

This effect can be explained when the rearrangement of charge carriers in the phosphor is considered. Within the context of persistent phosphors, two types of centers will undergo changes during excitation: the activators and the traps. The former will be ionized and simultaneously the charge will be trapped by the latter, turning the initially nonabsorbing defect into an optically active center which is susceptible to optically stimulated detrapping. It is not uncommon that crystalline defects introduce additional absorption bands after the capture of a charge carrier. If this is caused by the absorption of light, as in the current case, this phenomenon is referred to as photochromism. It is known to occur in numerous organic and inorganic materials, of which many are Eu-activated phosphors.[52−58] From this list, $CaAl_2O_4:Eu^{2+},Nd^{3+}$ is also known as a persistent phosphor, but in contrast to the case of $SrAl_2O_4:Eu^{2+},Dy^{3+}$ it seems that the absorption bands of the color center do not show overlap with the absorption bands of the Eu^{2+} activator, although it is yet unclear whether the color centers in $CaAl_2O_4:Eu^{2+},Nd^{3+}$ are also responsible for the trapping related to the persistent luminescence as is the case for $SrAl_2O_4:Eu^{2+},Dy^{3+}$.[53]

In case of $SrAl_2O_4:Eu^{2+},Dy^{3+}$, the strongly absorbing Eu^{2+} will be ionized to Eu^{3+},[59] which has a much lower absorption strength for the pumping wavelengths.[60,61] It is therefore reasonable to assume that the contribution of Eu^{3+} to the overall absorption can be neglected. Further assuming that the absorption of the empty traps is also negligible compared to the absorption of the other centers allows to write the average absorption per europium center as

$$f \times a_{tr} + (1 - f) \times a_{Eu^{2+}} \quad (2)$$

where a_{tr} and $a_{Eu^{2+}}$ represent the absorption of the filled traps and Eu^{2+}, respectively, as shown in Figure 1c, while f represents

DOI: 10.1021/acsphotonics.8b00979
ACS Photonics 2018, 5, 4529−4537

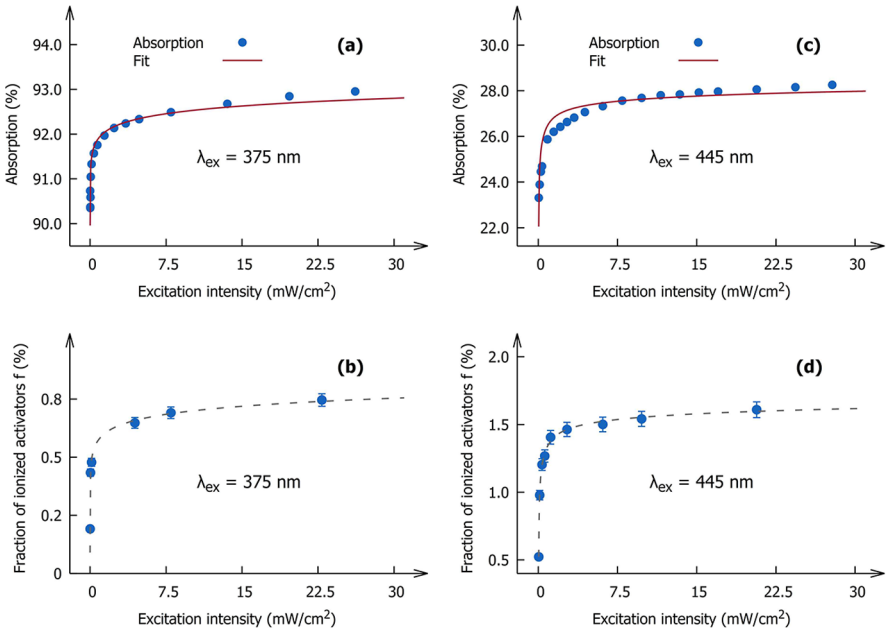

Figure 5. Absorption (a, c) and the fraction of ionized activator centers (b, d) of the phosphor as a function of the excitation intensity for 375 and 445 nm excitation, respectively. The red lines accompanying the absorption measurements (a, c) represent the fit based on eq 2, whereas the gray lines in (b, c) are merely guides to the eye. Note the similarities between the fraction of ionized europium centers and the fit to the absorption measurement, which is a direct consequence of the fact that the expression for the absorption in eq 2 is directly related to *f*.

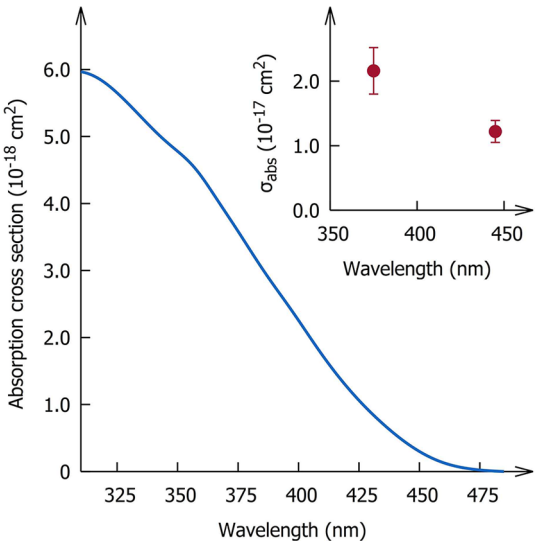

Figure 6. Absorption cross section of the $4f^7$ to $4f^65d^1$ transition of Eu^{2+} in $SrAl_2O_4:Eu^{2+},Dy^{3+}$. The inset shows the fitted absorption cross sections of the filled trap at 375 and 445 nm.

the fraction of ionized europium centers under conditions of dynamic equilibrium.

Since every photon emitted after excitation has stopped is originating from a previously trapped charge, the fraction of ionized activators *f* can be determined by counting the number of photons that are emitted during the afterglow. This technique was introduced in previous work, where the storage capacity of $SrAl_2O_4:Eu^{2+},Dy^{3+}$ was determined by measuring afterglow curves on samples with different phosphor loadings.[41] By performing these measurements on a single sample but for different excitation intensities, the intensity dependence of the storage capacity can be obtained. Combining this with the known activator concentrations yields the intensity dependence of the fraction f, which is shown in Figure 5b,d. This fraction levels off around 0.8% in case of 375 nm excitation and around 1.6% for 445 nm excitation.

The measured intensity dependence of *f* can be plugged into eq 2 to yield the intensity dependence of the absorption, which should hence show a very similar behavior to the intensity dependence of *f* itself, as can be seen from Figure 5. Fitting eq 2 to the measured intensity dependence of the absorption allows to empirically determine $a_{tr}/a_{Eu^{2+}}$. The result of this fit is shown in Figure 5a,c and yields a ratio $a_{tr}/a_{Eu^{2+}}$ of 6 ± 1 and 29 ± 4 upon excitation with 375 and 445 nm, respectively.

The strong wavelength dependence of this ratio can be explained by considering the absorption cross section of Eu^{2+}, a quantity that is independent of the sample geometry and is defined as

$$\sigma_{abs} = \alpha/N \tag{3}$$

in which α is the absorption coefficient (in cm^{-1}) and *N* represents the density of Eu^{2+} centers in the phosphor layer (in cm^{-3}). The absorption coefficient α was determined by measuring the diffuse transmission spectra of the transparent phosphor layers.[41] A polymer layer with a phosphor loading of 8 mg/cm^2 was chosen because of its negligible scattering, allowing to take the optical path length equal to the thickness of the phosphor layer. The absorption cross section of a phosphor layer in which the traps are all empty is displayed in Figure 6 from which it can be concluded that the absorption at 375 nm is about 8× higher compared to the absorption at 445 nm, which is in accordance with the difference in ratios. Remaining discrepancies can be due to the absorption cross section of the filled traps, which is also expected to have a wavelength dependence.

Nonetheless, the ratio $a_{tr}/a_{Eu^{2+}}$ is found to be bigger than unity for both excitation wavelengths. This implies that the absorption due to a filled trap is significantly higher than the absorption of a Eu^{2+} center. Upon comparison with the

DOI: 10.1021/acsphotonics.8b00979
ACS Photonics 2018, 5, 4529−4537

absorption cross section of Eu^{2+} in Figure 6, it is clear that the absorption cross sections of a filled trap are $(2.16 \pm 0.36) \times 10^{-17}$ cm^2 and $(1.22 \pm 0.17) \times 10^{-17}$ cm^2 for 375 and 445 nm excitation, respectively. Although this is quite high, it is not uncommon for intrinsic defects such as F-centers.[62−65] Tydtgat et al.[66] found a ratio of 228 for $Sr_2MgSi_2O_7$:Eu^{2+},Dy^{3+} and although this high value indicates the importance of the filled traps in the absorption process, it is likely overestimated. The value of 6−29 was obtained here by directly measuring the absorption, while the value of 228 was indirectly derived from charging and luminescence decay curves, necessitating the use of models, which might be inadequate to grasp the full details of the complex dynamics of persistent phosphors. Nevertheless, the high absorption of filled traps has important implications for the total amount of energy that can be stored in a persistent phosphor and its photoluminescence quantum efficiency.

The fact that the storage capacity of persistent phosphors is limited by OSL is in stark contrast with the common supposition that it is only limited by the number of activator centers that have access to traps. It is usually assumed that a fraction of the activators does not take part in the trapping process and that the size of this fraction is the limiting factor of the storage capacity. The activators that do not engage in the trapping process will nevertheless give rise to photoluminescence. This implies that the presence of such an inactive fraction would manifest itself as a nonzero offset at the beginning of the charging curves of a completely empty persistent phosphor. An example of such a charging curve is shown in Figure 7. It can be seen that the offset is small,

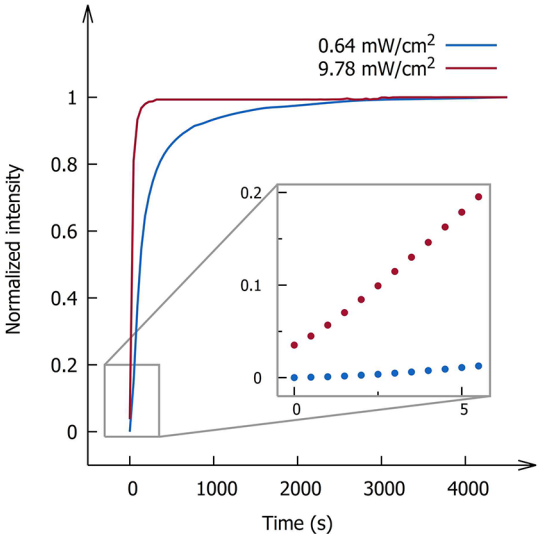

Figure 7. Charging curves of $SrAl_2O_4$:Eu^{2+},Dy^{3+} under 445 nm excitation. The inset shows the beginning of the curves in detail.

indicating that the fraction of activators that do not participate in the trapping processes is negligible. For a high excitation intensity of 10 mW/cm^2, a small offset is visible that can be attributed to a combination of the limited time resolution (0.5 s) of the equipment and the inherently faster charging behavior. Therefore, it can be stated that the main mechanism that limits the storage capacity of $SrAl_2O_4$:Eu^{2+},Dy^{3+} is indeed the OSL by excitation light.

Notwithstanding its simplicity, the model introduced in eq 2 can also account for the intensity dependence of the quantum efficiency. To illustrate this, a numerical simulation was performed. The simulated system is comprised of a set of Eu ions, each of which is coupled to a unique local trap. For simplicity, all processes are assumed to take place with 100% efficiency. The activator-trap complexes can assume one of two different states which are characterized by a fixed value for the absorption. Either the activator is not ionized and the trap is empty, in which case the absorption of the complex is equal to $a_{Eu^{2+}}$, or the activator is ionized in which case the trap is filled and the absorption is equal to a_{tr}. To simulate the effect of the excitation light on the system, a fixed number of the activator-trap complexes are forced to change state during every step of the simulation, thereby introducing trapping or optically stimulated detrapping. The fraction of the absorbed light used for either of these two processes is proportional to each species' contribution to the overall absorption. Afterglow is introduced into the simulation by allowing filled traps to be emptied spontaneously during every step. Finally, the arbitrary units of the simulation must be converted to physically meaningful units. The physical time that can be assigned to every simulation step can be determined by comparing the simulated charging curves in Figure 8a, with the experimental ones in Figure 7. Furthermore, the number of simulated Eu centers has to be compared to the number of Eu centers that are present in the layers that were characterized, allowing to determine the number of optical centers that change state during every simulation step. Because an equivalent number of photons is needed to induce these changes, this finally allows to express the excitation intensity in radiometric units. The only point at which a wavelength dependence is introduced into the simulation is when this photon flux is converted into an energy flux. The results shown in Figure 8 are thus valid for all excitation wavelengths but the values on the abscissa are valid only for excitation with 445 nm light. This was done to enable the comparison with the measurements shown in previous figures but the results can easily be generalized to other wavelengths by considering the energy difference between the photons.

Every simulation starts in a completely depleted state, meaning that all the traps are empty. Fixed values are chosen for the excitation intensity, the absorption of the activator centers and the absorption of the filled traps. As the simulation progresses in time more and more traps are filled until the system reaches a dynamic equilibrium. At this point, the simulated quantum efficiencies are calculated, in analogy with the above experiments. By repeating these simulations for different excitation intensities, the intensity dependence of the quantum efficiency and the trapping capacity is simulated. The results of the simulation are shown in Figure 8 from which it can be seen that the introduction of a nonzero absorption for the filled traps indeed leads to a decrease of the quantum efficiency and results in a storage capacity that is lower than 100%. The higher the value of $a_{tr}/a_{Eu^{2+}}$, the faster the system settles at a constant quantum efficiency and the lower the storage capacity becomes. A comparison of the simulated quantum efficiency with the data displayed in Figure 2 confirms that the ratio $a_{tr}/a_{Eu^{2+}}$ is indeed larger than unity and is, in fact, of the order of 1−10. The simulated storage capacity is systematically higher than the experimental values shown in Figure 5b,d, which can be explained by remembering that, in contrast to the simulated system, the phosphor has an overall quantum efficiency which is lower than unity thereby introducing extra losses. Looking at the above discussion it is

DOI: 10.1021/acsphotonics.8b00979
ACS Photonics 2018, 5, 4529−4537

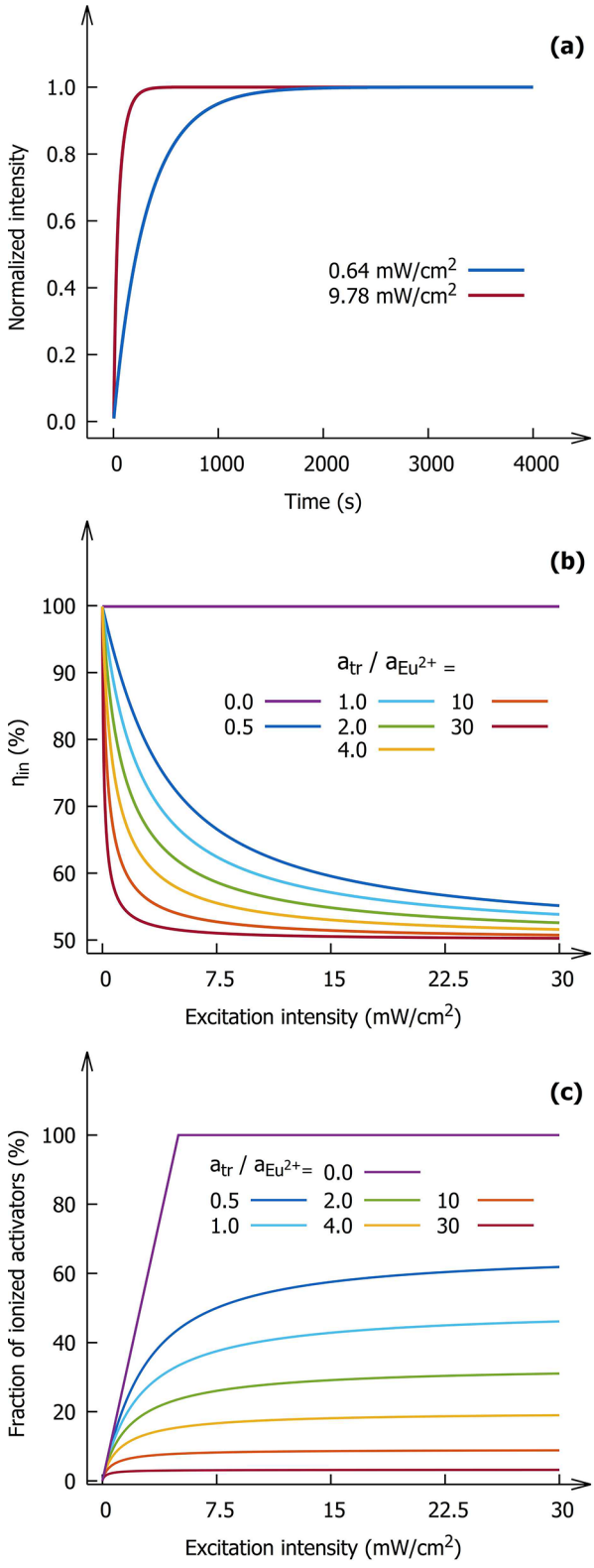

Figure 8. Results of the simulation. The charging curves (a) were simulated under the same excitation conditions (445 nm excitation) as the measurements in Figure 7. The intensity dependence of the internal quantum efficiency (b) and of the fraction of ionized activator centers (c) was simulated for different values of $a_{tr}/a_{Eu^{2+}}$.

clear that the agreement between the model and the data is not perfect. This is not surprising if the simplicity of the model is considered. It is tacitly assumed that only one trap depth is present in the phosphor, but the presence of multiple traps depths or even trap depth distributions has been reported for a variety of persistent phosphors, including $SrAl_2O_4:Eu^{2+},Dy^{3+}$, which is the subject of this investigation.[67,68]

High irradiances up to 1 W/cm^2 are readily encountered in present-day solid state lighting applications.[15,69] Therefore, the presence of traps in a LED phosphor should be handled with great consideration. Sometimes traps are deliberately incorporated into the phosphor. This is, for example, the case for persistent or storage phosphors. On the other hand, the presence of traps in LED phosphors is likely unintentional and could originate from defects that are introduced during synthesis.[39,70−72] In light of the above results, it can be concluded that the efficiency of a phosphor can be further optimized by carefully eliminating trapping centers. At the very least, the intensity dependence of the quantum efficiency makes it imperative that LED phosphors are tested under the same physical circumstances as those encountered in the intended application.

CONCLUSION

The intensity dependence of the quantum efficiency of $SrAl_2O_4:Eu^{2+},Dy^{3+}$ was measured. It is found that the efficiency significantly decreases with increasing excitation intensity. This effect is attributed to the occurrence of OSL by excitation light during charging. It is found that this decrease in efficiency is accompanied by an increase of the absorption of the phosphor. A simple model, consisting of two different optically active centers, is used to demonstrate that the absorption of filled traps is larger than the absorption of Eu^{2+}, which implies that optically stimulated detrapping is favored over trapping or photoluminescence.

From the point of view of persistent phosphors it is clear that this effect limits their storage capacity, since it opens up an additional pathway for detrapping during excitation. This implies that the absorption characteristics of the trap should be taken into account when engineering new persistent phosphors. On the other hand it is found that the presence of traps lowers a phosphor's quantum efficiency. Careful elimination of possible trapping centers in LED phosphors might, therefore, offer a way to further increase the quantum efficiency of LED phosphors.

AUTHOR INFORMATION

Corresponding Author

*E-mail: philippe.smet@ugent.be. Tel.: +32 9 264 43 53.

ORCID

David Van der Heggen: 0000-0002-6938-5573

Jonas J. Joos: 0000-0002-7869-2217

Philippe F. Smet: 0000-0003-4789-5799

Funding

D.V.d.H. and J.J.J. are grateful to the UGent Special Research Fund (BOF) for financial support (BOF16/DOC/327 and BOF/PDO/2017/002101). P.F.S. acknowledges the BOF GOA Project ENCLOSE.

Notes

The authors declare no competing financial interest.

ACKNOWLEDGMENTS

The authors would like to thank Claude Tydtgat for carefully reading the manuscript and offering constructive feedback.

DOI: 10.1021/acsphotonics.8b00979
ACS Photonics 2018, 5, 4529−4537

REFERENCES

(1) Smet, P. F.; Parmentier, A. B.; Poelman, D. Selecting Conversion Phosphors for White Light-Emitting Diodes. *J. Electrochem. Soc.* **2011**, *158* (6), R37−R54.

(2) Chen, L.; Lin, C.-C.; Yeh, C.-W.; Liu, R.-S. Light Converting Inorganic Phosphors for White Light-Emitting Diodes. *Materials* **2010**, *3* (3), 2172−2195.

(3) Pust, P.; Weiler, V.; Hecht, C.; Tücks, A.; Wochnik, A. S.; Henß, A.-K.; Wiechert, D.; Scheu, C.; Schmidt, P. J.; Schnick, W. Narrow-Band Red-Emitting $Sr[LiAl_3N_4]:Eu^{2+}$ as a next-Generation LED-Phosphor Material. *Nat. Mater.* **2014**, *13* (9), 891−896.

(4) Xia, Z.; Xu, Z.; Chen, M.; Liu, Q. Recent Developments in the New Inorganic Solid-State LED Phosphors. *Dalt. Trans.* **2016**, *45* (28), 11214−11232.

(5) Xia, Z.; Liu, Q. Progress in Discovery and Structural Design of Color Conversion Phosphors for LEDs. *Prog. Mater. Sci.* **2016**, *84*, 59−117.

(6) Arias, M.; Vázquez, A.; Sebastián, J. An Overview of the AC-DC and DC-DC Converters for LED Lighting Applications. *Automatika* **2012**, *53* (2), 156−172.

(7) Yen, H.-H.; Yeh, W.-Y.; Kuo, H.-C. GaN Alternating Current Light-Emitting Device. *Phys. Status Solidi A* **2007**, *204* (6), 2077−2081.

(8) Onushkin, G. A.; Lee, Y.-J.; Yang, J.-J.; Kim, H.-K.; Son, J.-K.; Park, G.-H.; Park, Y.-J. Efficient Alternating Current Operated White Light-Emitting Diode Chip. *IEEE Photonics Technol. Lett.* **2009**, *21* (1), 33−35.

(9) Wilkins, A.; Veitch, J.; Lehman, B. LED Lighting Flicker and Potential Health Concerns: IEEE Standard PAR1789 Update. In *2010 IEEE Energy Conversion Congress and Exposition*; IEEE, 2010; pp 171−178.

(10) Setlur, A. A.; Shiang, J. J.; Happek, U. Eu^{2+}-Mn^{2+} Phosphor Saturation in 5 Mm Light Emitting Diode Lamps. *Appl. Phys. Lett.* **2008**, *92* (8), 081104.

(11) Sijbom, H. F.; Verstraete, R.; Joos, J. J.; Poelman, D.; Smet, P. F. $K_2SiF_6:Mn^{4+}$ as a Red Phosphor for Displays and Warm-White LEDs: A Review of Properties and Perspectives. *Opt. Mater. Express* **2017**, *7* (9), 3332−3365.

(12) Korte, S.; Lindfeld, E.; Jüstel, T. Flicker Reduction of AC LEDs by Mn^{2+} Doped Apatite Phosphor. *ECS J. Solid State Sci. Technol.* **2018**, *7* (3), R21−R26.

(13) Song, E.; Zhou, Y.; Yang, X.-B.; Liao, Z.; Zhao, W.; Deng, T.; Wang, L.; Ma, Y.; Ye, S.; Zhang, Q. Highly Efficient and Stable Narrow-Band Red Phosphor $Cs_2SiF_6:Mn^{4+}$ for High-Power Warm White LED Applications. *ACS Photonics* **2017**, *4* (10), 2556−2565.

(14) Sijbom, H. F.; Joos, J. J.; Martin, L. I. D. J.; Van den Eeckhout, K.; Poelman, D.; Smet, P. F. Luminescent Behavior of the $K_2SiF_6:Mn^{4+}$ Red Phosphor at High Fluxes and at the Microscopic Level. *ECS J. Solid State Sci. Technol.* **2016**, *5* (1), R3040−R3048.

(15) Bicanic, K. T.; Li, X.; Sabatini, R. P.; Hossain, N.; Wang, C.-F.; Fan, F.; Liang, H.; Hoogland, S.; Sargent, E. H. Design of Phosphor White Light Systems for High-Power Applications. *ACS Photonics* **2016**, *3* (12), 2243−2248.

(16) Lin, H.; Wang, B.; Xu, J.; Zhang, R.; Chen, H.; Yu, Y.; Wang, Y. Phosphor-in-Glass for High-Powered Remote-Type White AC-LED. *ACS Appl. Mater. Interfaces* **2014**, *6* (23), 21264−21269.

(17) Lin, H.; Xu, J.; Huang, Q.; Wang, B.; Chen, H.; Lin, Z.; Wang, Y. Bandgap Tailoring via Si Doping in Inverse-Garnet $Mg_3Y_2Ge_3O_{12}:Ce^{3+}$ Persistent Phosphor Potentially Applicable in AC-LED. *ACS Appl. Mater. Interfaces* **2015**, *7* (39), 21835−21843.

(18) Chen, L.; Zhang, Y. S.; Xue, C.; Deng, X. R.; Luo, A. Q.; Liu, F. Y.; Jiang, Y. The Green Phosphor $SrAl_2O_4:Eu^{2+}$, R^{3+} (R = Y,Dy) and Its Application in Alternating Current Light-Emitting Diodes. *Funct. Mater. Lett.* **2013**, *06* (04), 1350047.

(19) Li, B.; Zhang, J.; Zhang, M.; Long, Y.; He, X. Effects of $SrCl_2$ as a Flux on the Structural and Luminescent Properties of $SrAl_2O_4:Eu^{2+}$, Dy^{3+} Phosphors for AC-LEDs. *J. Alloys Compd.* **2015**, *651*, 497−502.

(20) Ueda, J.; Kuroishi, K.; Tanabe, S. Yellow Persistent Luminescence in Ce^{3+}-Cr^{3+}-Codoped Gadolinium Aluminum Gallium Garnet Transparent Ceramics after Blue-Light Excitation. *Appl. Phys. Express* **2014**, *7* (6), 062201.

(21) Liu, Y.-F.; Liu, P.; Wang, L.; Cui, C.-E.; Jiang, H.-C.; Jiang, J. A Two-Step Solid-State Reaction to Synthesize the Yellow Persistent $Gd_3Al_2Ga_3O_{12}:Ce^{3+}$ Phosphor with an Enhanced Optical Performance for AC-LEDs. *Chem. Commun.* **2017**, *53* (77), 10636−10639.

(22) Yeh, C.-W.; Li, Y.; Wang, J.; Liu, R.-S. Appropriate Green Phosphor of $SrSi_2O_2N_2:Eu^{2+},Mn^{2+}$ for AC LEDs. *Opt. Express* **2012**, *20* (16), 18031−18043.

(23) Miranda de Carvalho, J.; Pedroso, C. C. S.; Machado, I. P.; Hölsä, J.; Rodrigues, L. C. V.; Głuchowski, P.; Lastusaari, M.; Brito, H. F. Persistent Luminescence Warm-Light LEDs Based on Ti-Doped RE_2O_2S Materials Prepared by Rapid and Energy-Saving Microwave-Assisted Synthesis. *J. Mater. Chem. C* **2018**, *6*, 8897−8905.

(24) Lin, H.; Wang, B.; Huang, Q.; Huang, F.; Xu, J.; Chen, H.; Lin, Z.; Wang, J.; Hu, T.; Wang, Y. $Lu_2CaMg_2(Si_{1-x}Ge_x)_3O_{12}:Ce^{3+}$ Solid-Solution Phosphors: Bandgap Engineering for Blue-Light Activated Afterglow Applicable to AC-LED. *J. Mater. Chem. C* **2016**, *4* (43), 10329−10338.

(25) Su, Q.; Li, C.; Wang, J. Some Interesting Phenomena in the Study of Rare Earth Long Lasting Phosphors. *Opt. Mater.* **2014**, *36* (11), 1894−1900.

(26) Van den Eeckhout, K.; Smet, P. F.; Poelman, D. Persistent Luminescence in Eu^{2+}-Doped Compounds: A Review. *Materials* **2010**, *3* (4), 2536−2566.

(27) Clabau, F.; Rocquefelte, X.; Jobic, S.; Deniard, P.; Whangbo, M.-H.; Garcia, A.; Le Mercier, T. Mechanism of Phosphorescence Appropriate for the Long-Lasting Phosphors Eu^{2+}-Doped $SrAl_2O_4$ with Codopants Dy^{3+} and B^{3+}. *Chem. Mater.* **2005**, *17* (15), 3904−3912.

(28) Aitasalo, T.; Hölsä, J.; Jungner, H.; Lastusaari, M.; Niittykoski, J. Thermoluminescence Study of Persistent Luminescence Materials: Eu^{2+}-and R^{3+}-Doped Calcium Aluminates, $CaAl_2O_4:Eu^{2+},R^{3+}$. *J. Phys. Chem. B* **2006**, *110*, 4589−4598.

(29) Dorenbos, P. Mechanism of Persistent Luminescence in Eu^{2+} and Dy^{3+} Codoped Aluminate and Silicate Compounds. *J. Electrochem. Soc.* **2005**, *152* (7), H107−H110.

(30) Xu, J.; Tanabe, S. Persistent Luminescence Instead of Phosphorescence: History, Mechanism, and Perspective. *J. Lumin.* **2018**, DOI: 10.1016/j.jlumin.2018.09.047.

(31) Bos, A. J. J. Theory of Thermoluminescence. *Radiat. Meas.* **2006**, *41*, S45−S56.

(32) Botterman, J.; Smet, P. F. Persistent Phosphor $SrAl_2O_4:Eu,Dy$ in Outdoor Conditions: Saved by the Trap Distribution. *Opt. Express* **2015**, *23* (15), A868−A881.

(33) Maldiney, T.; Lecointre, A.; Viana, B.; Bessière, A.; Bessodes, M.; Gourier, D.; Richard, C.; Scherman, D. Controlling Electron Trap Depth To Enhance Optical Properties of Persistent Luminescence Nanoparticles for In Vivo Imaging. *J. Am. Chem. Soc.* **2011**, *133* (30), 11810−11815.

(34) Rodríguez Burbano, D. C.; Sharma, S. K.; Dorenbos, P.; Viana, B.; Capobianco, J. A. Persistent and Photostimulated Red Emission in $CaS:Eu^{2+},Dy^{3+}$ Nanophosphors. *Adv. Opt. Mater.* **2015**, *3* (4), 551−557.

(35) Leblans, P.; Vandenbroucke, D.; Willems, P. Storage Phosphors for Medical Imaging. *Materials* **2011**, *4* (6), 1034−1086.

(36) Liu, F.; Yan, W.; Chuang, Y.-J.; Zhen, Z.; Xie, J.; Pan, Z. Photostimulated Near-Infrared Persistent Luminescence as a New Optical Read-out from Cr^{3+}-Doped $LiGa_5O_8$. *Sci. Rep.* **2013**, *3* (1), 1554.

(37) Kim, Y. H.; Arunkumar, P.; Kim, B. Y.; Unithrattil, S.; Kim, E.; Moon, S.-H.; Hyun, J. Y.; Kim, K. H.; Lee, D.; Lee, J.-S.; et al. A Zero-Thermal-Quenching Phosphor. *Nat. Mater.* **2017**, *16* (5), 543−550.

(38) Qiao, J.; Ning, L.; Molokeev, M. S.; Chuang, Y.-C.; Liu, Q.; Xia, Z. Eu^{2+} Site Preferences in the Mixed Cation $K_2BaCa(PO_4)_2$ and Thermally Stable Luminescence. *J. Am. Chem. Soc.* **2018**, *140* (30), 9730−9736.

DOI: 10.1021/acsphotonics.8b00979
ACS Photonics 2018, 5, 4529−4537

(39) Xia, Z.; Meijerink, A. Ce^{3+}-Doped Garnet Phosphors: Composition Modification, Luminescence Properties and Applications. *Chem. Soc. Rev.* **2017**, *46* (1), 275−299.
(40) Smet, P. F.; Joos, J. J. White Light-Emitting Diodes: Stabilizing Colour and Intensity. *Nat. Mater.* **2017**, *16* (5), 500−501.
(41) Van der Heggen, D.; Joos, J. J.; Rodríguez Burbano, D.; Capobianco, J.; Smet, P. F. Counting the Photons: Determining the Absolute Storage Capacity of Persistent Phosphors. *Materials* **2017**, *10* (8), 867.
(42) Abe, S.; Joos, J. J.; Martin, L. I.; Hens, Z.; Smet, P. F. Hybrid Remote Quantum Dot/Powder Phosphor Designs for Display Backlights. *Light: Sci. Appl.* **2017**, *6* (6), e16271.
(43) Bachmann, V.; Ronda, C.; Meijerink, A. Temperature Quenching of Yellow Ce^{3+} Luminescence in YAG:Ce. *Chem. Mater.* **2009**, *21* (10), 2077−2084.
(44) Chen, Z.; Zhu, Y.; Guo, X.; Li, M.; Ge, M. Comparison of the Luminescent Properties of Warm-Toned Long-Lasting Phosphorescent Composites: SiO_2Red-Emitting Color Converter@SrAl_2O_4:Eu^{2+},Dy^{3+} and PMMA/Red-Emitting Color Converter@ SrAl_2O_4:Eu^{2+},Dy^{3+}. *J. Lumin.* **2018**, *199*, 1−5.
(45) Botterman, J.; Joos, J. J.; Smet, P. F. Trapping and Detrapping in $SrAl_2O_4$:Eu,Dy Persistent Phosphors: Influence of Excitation Wavelength and Temperature. *Phys. Rev. B: Condens. Matter Mater. Phys.* **2014**, *90* (8), 085147.
(46) Ning, L.; Huang, X.; Huang, Y.; Tanner, P. A. Origin of Green Persistent Luminescence of Eu-Doped $SrAl_2O_4$ from Multiconfigurational Ab Initio Study of $4f^7$-$4f^65d^1$ Transitions. *J. Mater. Chem. C* **2018**, *6*, 6637−6640.
(47) Bierwagen, J.; Yoon, S.; Gartmann, N.; Walfort, B.; Hagemann, H. Thermal and Concentration Dependent Energy Transfer of Eu^{2+} in $SrAl_2O_4$. *Opt. Mater. Express* **2016**, *6* (3), 793−803.
(48) Nazarov, M.; Brik, M. G.; Spassky, D.; Tsukerblat, B. Crystal Field Splitting of 5d States and Luminescence Mechanism in $SrAl_2O_4$:Eu^{2+} Phosphor. *J. Lumin.* **2017**, *182*, 79−86.
(49) Auzel, F. Upconversion and Anti-Stokes Processes with f and d Ions in Solids. *Chem. Rev.* **2004**, *104* (1), 139−174.
(50) Pollnau, M.; Gamelin, D. R.; Lüthi, S. R.; Güdel, H. U.; Hehlen, M. P. Power Dependence of Upconversion Luminescence in Lanthanide and Transition-Metal-Ion Systems. *Phys. Rev. B: Condens. Matter Mater. Phys.* **2000**, *61* (5), 3337−3346.
(51) Yoon, S.; Bierwagen, J.; Trottmann, M.; Walfort, B.; Gartmann, N.; Weidenkaff, A.; Hagemann, H.; Pokrant, S. The Influence of Boric Acid on Improved Persistent Luminescence and Thermal Oxidation Resistance of $SrAl_2O_4$:Eu^{2+}. *J. Lumin.* **2015**, *167*, 126−131.
(52) Hommel, D.; Langer, J. M.; Krukowska-Fulde, B. Thermoluminescence and Photochromism of CdF_2:Eu. *Phys. Status Solidi* **1975**, *31* (1), K81−K84.
(53) Ueda, J.; Shinoda, T.; Tanabe, S. Photochromism and Near-Infrared Persistent Luminescence in Eu^{2+}-Nd^{3+}-Co-Doped $CaAl_2O_4$ Ceramics. *Opt. Mater. Express* **2013**, *3* (6), 787.
(54) Akiyama, M. Blue-Green Light Photochromism in Europium Doped $BaMgSiO_4$. *Appl. Phys. Lett.* **2010**, *97* (18), 181905.
(55) Lv, Y.; Jin, Y.; Wang, C.; Ju, G.; Xue, F.; Hu, Y. Reversible White-Purple Photochromism in Europium Doped $Sr_3GdLi(PO_4)_3F$ Powders. *J. Lumin.* **2017**, *186*, 238−242.
(56) Ju, G.; Hu, Y.; Chen, L.; Wang, X. Photochromism of Europium and Gadolinium Co-Doped Barium Haloapatite. *ECS Solid State Lett.* **2012**, *1* (1), R1−R3.
(57) Misra, N.; Roy, M.; Mohanta, D.; Baruah, K.; Choudhury, A. Photochromism and Magneto-Optic Response of ZnO:Mn Semiconductor Quantum Dots Fabricated by Microemulsion Route. *Open Phys.* **2008**, *6* (1), 109−115.
(58) Ramaz, F.; Hamri, A.; Briat, B.; Topa, V.; Mitroaica, G. Magnetic Circular Dichroism and Absorption Study of Photochromism in Mn-Doped $Bi_{12}GeO_{20}$. *Radiat. Eff. Defects Solids* **1995**, *136* (1−4), 99−102.
(59) Korthout, K.; Van den Eeckhout, K.; Botterman, J.; Nikitenko, S.; Poelman, D.; Smet, P. F. Luminescence and X-Ray Absorption Measurements of Persistent $SrAl_2O_4$:Eu,Dy Powders: Evidence for Valence State Changes. *Phys. Rev. B: Condens. Matter Mater. Phys.* **2011**, *84* (8), 085140.
(60) Poort, S. H. M.; Meyerink, A.; Blasse, G. Lifetime Measurements in Eu^{2+}-Doped Host Lattices. *J. Phys. Chem. Solids* **1997**, *58* (9), 1451−1456.
(61) Görller-Walrand, C.; Binnemans, K. Spectral Intensities of F-f Transitions. In *Handbook on the Physics and Chemistry of Rare Earths*; Elsevier, 1998; Vol. *25*, Chapter 167, pp 101−264.
(62) Von Seggern, H.; Voigt, T.; Knüpfer, W.; Lange, G. Physical Model of Photostimulated Luminescence of X-Ray Irradiated BaFBr:Eu^{2+}. *J. Appl. Phys.* **1988**, *64* (3), 1405−1412.
(63) De Leeuw, D. M.; Kovats, T.; Herko, S. P. Kinetics of Photostimulated Luminescence in BaFBr:Eu. *J. Electrochem. Soc.* **1987**, *134*, 491−492.
(64) Basiev, T. T.; Mirov, S. B.; Osiko, V. V. Room-Temperature Color Center Lasers. *IEEE J. Quantum Electron.* **1988**, *24* (6), 1052−1069.
(65) von Seggern, H. Photostimulable X-Ray Storage Phosphors: A Review of Present Understanding. *Braz. J. Phys.* **1999**, *29* (2), 254−268.
(66) Tydtgat, C.; Meert, K. W.; Poelman, D.; Smet, P. F. Optically Stimulated Detrapping during Charging of Persistent Phosphors. *Opt. Mater. Express* **2016**, *6* (3), 844.
(67) Hagemann, H.; Lovy, D.; Yoon, S.; Pokrant, S.; Gartmann, N.; Walfort, B.; Bierwagen, J. Wavelength Dependent Loading of Traps in the Persistent Phosphor $SrAl_2O_4$:Eu^{2+}, Dy^{3+}. *J. Lumin.* **2016**, *170*, 299−304.
(68) Van den Eeckhout, K.; Bos, A. J. J.; Poelman, D.; Smet, P. F. Revealing Trap Depth Distributions in Persistent Phosphors. *Phys. Rev. B: Condens. Matter Mater. Phys.* **2013**, *87* (4), 045126.
(69) Krames, M. R.; Shchekin, O. B.; Mueller-Mach, R.; Mueller, G. O.; Zhou, L.; Harbers, G.; Craford, M. G. Status and Future of High-Power Light-Emitting Diodes for Solid-State Lighting. *J. Disp. Technol.* **2007**, *3* (2), 160−175.
(70) Li, Y. Q.; van Steen, J. E. J.; van Krevel, J. W. H.; Botty, G.; Delsing, A. C. A.; DiSalvo, F. J.; de With, G.; Hintzen, H. T. Luminescence Properties of Red-Emitting $M_2Si_5N_8$:Eu^{2+} (M = Ca, Sr, Ba) LED Conversion Phosphors. *J. Alloys Compd.* **2006**, *417* (1−2), 273−279.
(71) Bachmann, V.; Ronda, C.; Oeckler, O.; Schnick, W.; Meijerink, A. Color Point Tuning for (Sr,Ca,Ba)$Si_2O_2N_2$:Eu^{2+} for White Light LEDs. *Chem. Mater.* **2009**, *21* (2), 316−325.
(72) Joos, J. J.; Botterman, J.; Smet, P. F. Evaluating the Use of Blue Phosphors in White LEDs: The Case of $Sr_{0.25}Ba_{0.75}Si_2O_2N_2$:$Eu^{2+}$. *J. Solid State Light.* **2014**, *1* (1), 6.

DOI: 10.1021/acsphotonics.8b00979
ACS Photonics 2018, 5, 4529−4537